

X-Ray Dose and Spot Size Calculations for the DARHT-II Distributed Target

J. McCarrick

April 5, 2001

U.S. Department of Energy

Lawrence
Livermore
National
Laboratory

DISCLAIMER

This document was prepared as an account of work sponsored by an agency of the United States Government. Neither the United States Government nor the University of California nor any of their employees, makes any warranty, express or implied, or assumes any legal liability or responsibility for the accuracy, completeness, or usefulness of any information, apparatus, product, or process disclosed, or represents that its use would not infringe privately owned rights. Reference herein to any specific commercial product, process, or service by trade name, trademark, manufacturer, or otherwise, does not necessarily constitute or imply its endorsement, recommendation, or favoring by the United States Government or the University of California. The views and opinions of authors expressed herein do not necessarily state or reflect those of the United States Government or the University of California, and shall not be used for advertising or product endorsement purposes.

This work was performed under the auspices of the U. S. Department of Energy by the University of California, Lawrence Livermore National Laboratory under Contract No. W-7405-Eng-48.

This report has been reproduced directly from the best available copy.

Available electronically at <http://www.doc.gov/bridge>

Available for a processing fee to U.S. Department of Energy
And its contractors in paper from
U.S. Department of Energy
Office of Scientific and Technical Information
P.O. Box 62
Oak Ridge, TN 37831-0062
Telephone: (865) 576-8401
Facsimile: (865) 576-5728
E-mail: reports@adonis.osti.gov

Available for the sale to the public from
U.S. Department of Commerce
National Technical Information Service
5285 Port Royal Road
Springfield, VA 22161
Telephone: (800) 553-6847
Facsimile: (703) 605-6900
E-mail: orders@ntis.fedworld.gov
Online ordering: <http://www.ntis.gov/ordering.htm>

OR

Lawrence Livermore National Laboratory
Technical Information Department's Digital Library
<http://www.llnl.gov/tid/Library.html>

X-Ray Dose and Spot Size Calculations for the DARHT-II Distributed Target

April 5, 2001

Jim McCarrick
Lawrence Livermore National Laboratory
P.O. Box 808, L-645
Livermore, CA 94551
(925) 423-8182 (office)
(925) 422-1767 (fax)
mccarrick1@llnl.gov

This work was performed under the auspices of the U.S. Department of Energy by the University of California, Lawrence Livermore National Laboratory under contract No. W-7405-Eng-48.

I. Introduction

The baseline DARHT-II converter target consists of foamed tantalum within a solid-density cylindrical tamper. The baseline design has been modified by D. Ho to further optimize the integrated line density of material in the course of multiple beam pulses. LASNEX simulations of the hydrodynamic expansion of the target have been performed by D. Ho (documented elsewhere). The resulting density profiles have been used as inputs in the MCNP radiation transport code to calculate the X-ray dose and spot size assuming an incoming Gaussian electron beam with $\sigma=0.65\text{mm}$, and a PIC-generated beam taking into account the “swept” spot emerging from the DARHT-II kicker system.

A prerequisite to these calculations is the absorption spectrum of air. In order to obtain this, a separate series of MCNP runs was performed for a set of monoenergetic photon sources, tallying the energy deposited in a volume of air. The forced collision feature was used to improve the statistics since the photon mean free path in air is extremely long at the energies of interest. A sample input file is given below. The resulting data for the MCNP DE and DF cards is shown in the beam-pulse input files, one of which is listed below. Note that the DE and DF cards are entered in column format for easy reading.

II. Simulation and Results

The geometry used to study the problem is shown in figure 1. The volumes within the tamper region have their densities set to the values calculated by LASNEX for each pulse. The resulting density profiles at the beginning of pulses 2, 3, and 4 are shown in figures 2-4. The DARHT-II beam is generated using the MCNP general source to produce a Gaussian at a waist, with a “flat” thermal profile with a maximum thermal angle corresponding to a normalized emittance of $1500\pi\text{-mm-mrad}$. This is the best possible representation within MCNP without using combined PIC/MCNP techniques, which require more time.

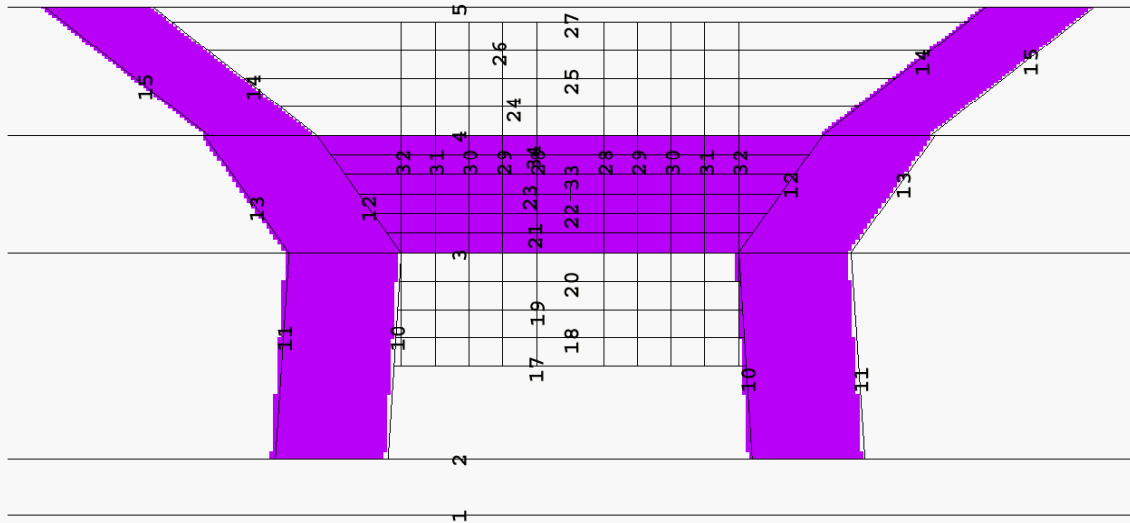


Figure 1. MCNP geometry for the modified foamed target configuration (D. Ho). The initial target is 0.42cm long, 1.5mm in radius on the upstream side, and has a density of 3.95 g/cc.

The output of the MCNP runs is the on-axis dose in air at one meter, per nanosecond of pulse at 2kA and 20MeV. This is multiplied by the pulse lengths to produce the results shown in figure 5. The total dose and that due only to photons in the 1-10 MeV range are tallied. Also, a perfect knife edge is placed one meter from the target and the X-ray shadow at two meters is measured with a vertical array of MCNP detector elements. The derivative of the shadow represents the effective X-ray spot, shown in figure 6. Figure 7 shows the results of fitting a Gaussian profile to these curves; note that the distributed target does result in moderate spot growth, up to 10% relative to the incoming electron beam; only 6% relative to the X-ray spot size at the first pulse. An examination of the LASNEX density profiles shows that the radial compression wave increases the apparent spot size by providing a heavier weighting of the outer parts of the electron beam. Note that no attenuation is assumed between the target and the one meter mark.

Several figures of merit can be examined to validate these results. The representation of the density profile in MCNP is somewhat crude but the integrated values are quite reasonable. The on-axis line density in the MCNP model is 1.28, 0.42, and 0.3 g/cc for pulses 2, 3, and 4 respectively; the corresponding LASNEX values are 1.0, 0.5, and 0.3. It seems surprising that the dose per ns at pulse 4 is 0.8 of the full value even though the on-axis line density has fallen to 0.2 of its nominal value. However, the volume-averaged and beam-weighted line density is 0.47. Comparing this value with a curve of energy flux produced versus line density (see figure 8) indeed shows that the flux is only down to 80% of the total. Thus the averaged line density could drop to as low as 0.16 g/cc and still meet the specifications for the fourth pulse.

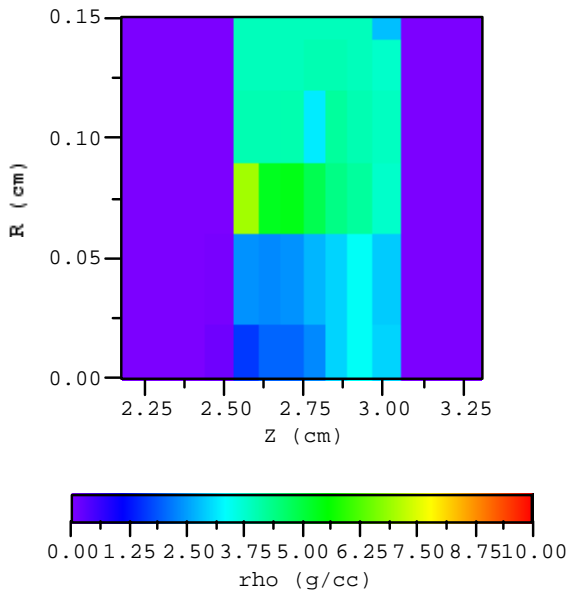


Figure 2. Density profile for pulse 2.

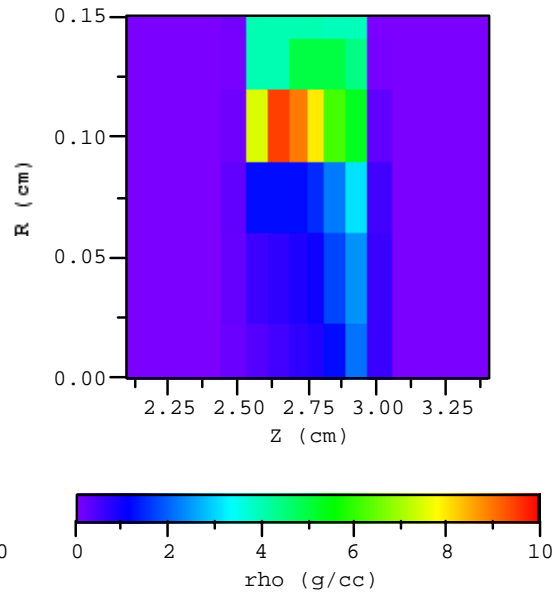


Figure 3. Density profile for pulse 3.

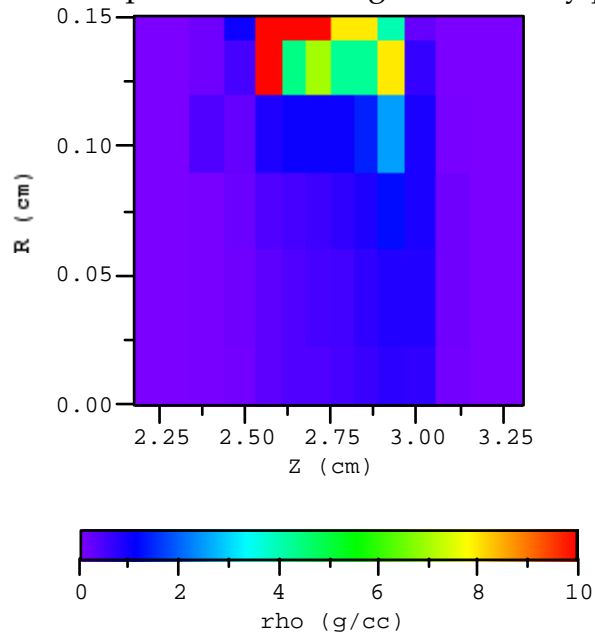


Figure 4. Density profile for pulse 4.

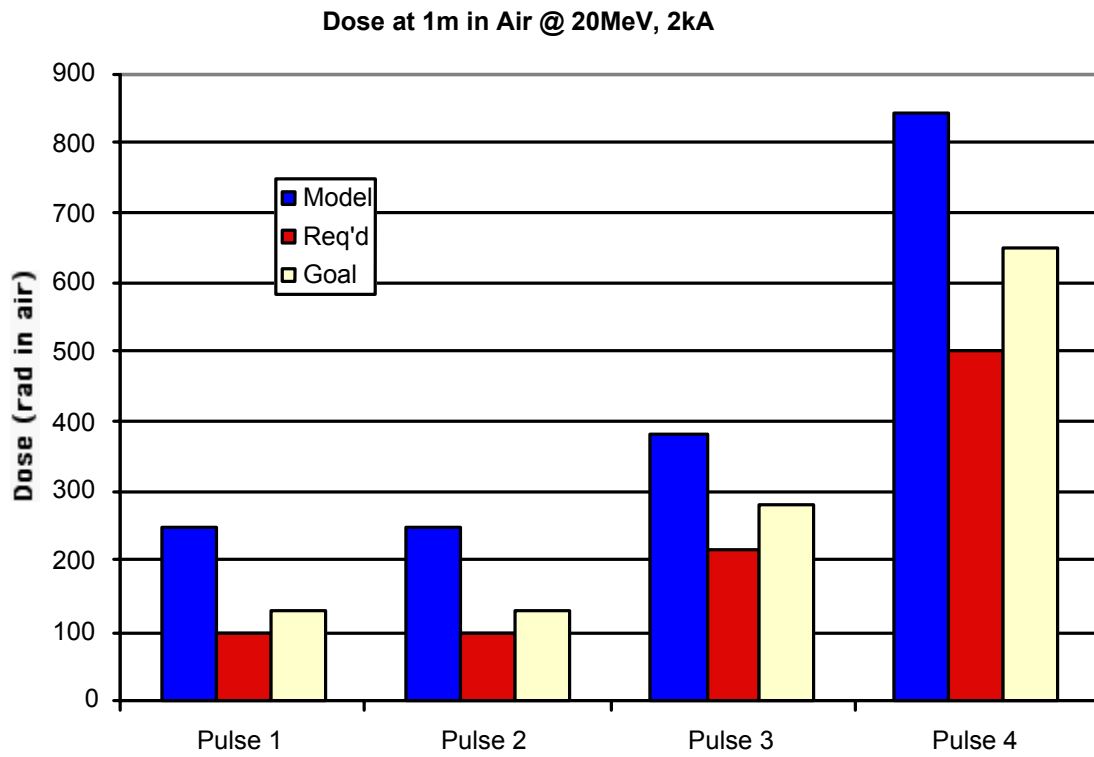


Figure 5. Dose in air at one meter; no attenuation after target.

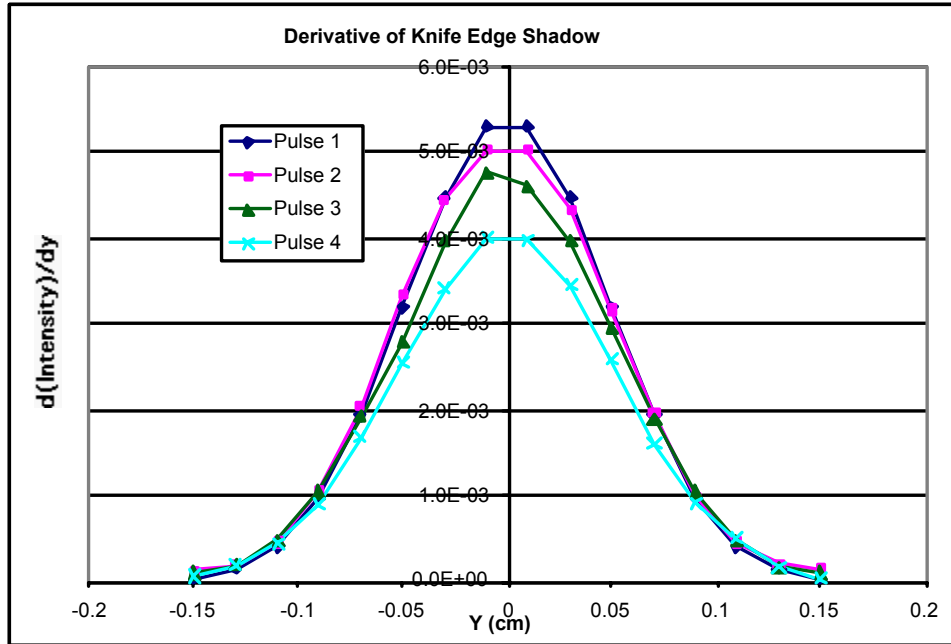


Figure 6. Derivative of the knife-edge shadow, showing X-ray spot resolution produced by the distributed target material.

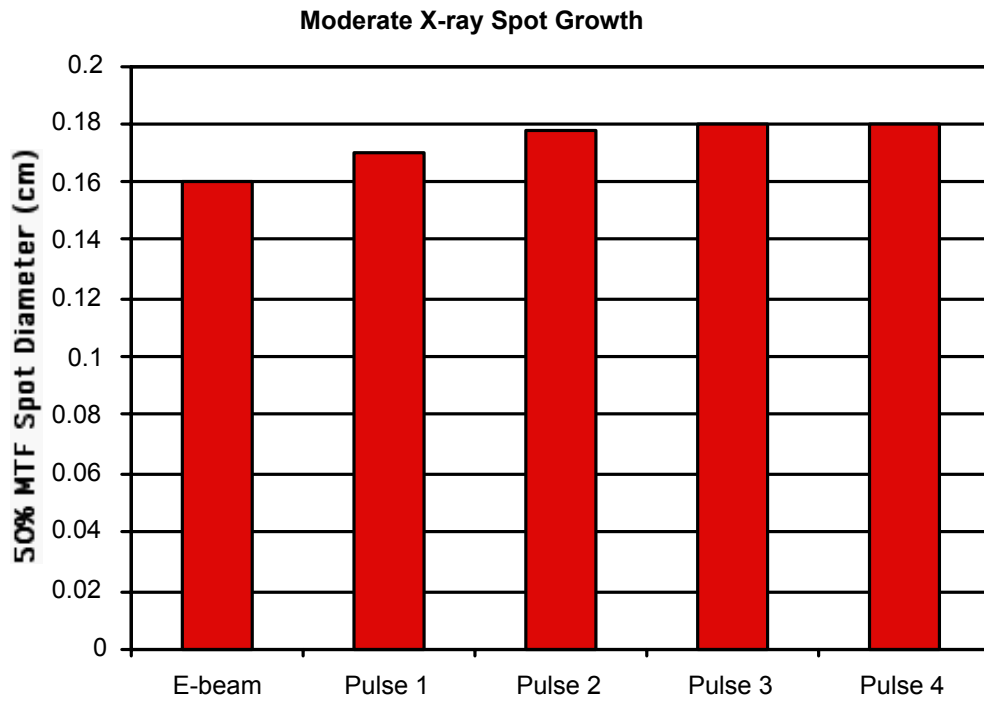


Figure 7. Gaussian fits to the above profiles, showing moderate spot growth.

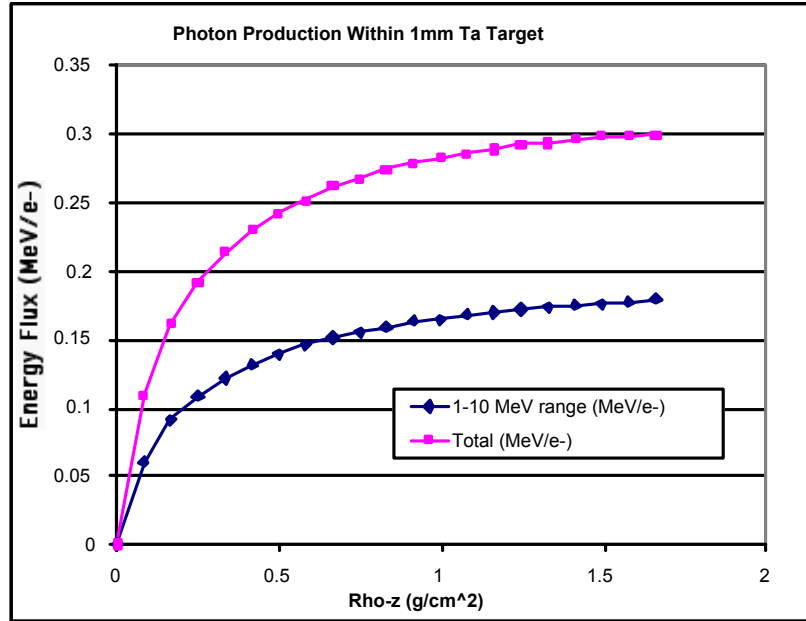


Figure 8. Integrated energy flux versus line density.

Another case with decidedly different behavior has been examined. A PIC representation of the “swept” beam profile resulting from the DARHT-II kicker system (provided by B. Poole) has been used as input in MCNP for similar dose and spot size calculations. These are done at a beam energy of 18.4 MeV; however, it should be noted that the density profiles used for each pulse are those corresponding to the 20 MeV Gaussian, since LASNEX data was not available for the swept case.

The dose calculation is shown in figure 9. The pulse lengths have been adjusted to compensate for the change in energy relative to 20 MeV. Despite this adjustment, the goal doses are no longer met by this non-ideal beam; the required dose is still obtained. There is some anomalous behavior: note that the dose rate (rad/ns) corresponding to the different pulses is not monotonic; it increases, then decreases.

The spot size behavior is also anomalous (see figure 10). The X-ray MTF sizes are smaller than that of the incoming electron beam. This is not, in general, impossible but does put constraints on the distribution of target material, requiring that the beam maintain positional/angular correlations in the presence of scattering. It is unlikely that this occurs in the target; it is more likely that this spot behavior is an artifact of using a density profile that was produced by a different beam distribution.

Finally, phase plots of this beam are shown in figures 11-13.

III. Conclusions

The radiographic performance of the foamed DARHT-II meets the multi-pulse dose requirements but requires some further investigation for spot size, due to possible effects of kicker sweep. Note that this statement takes the LASNEX-generated hydrodynamic performance as a “given.”

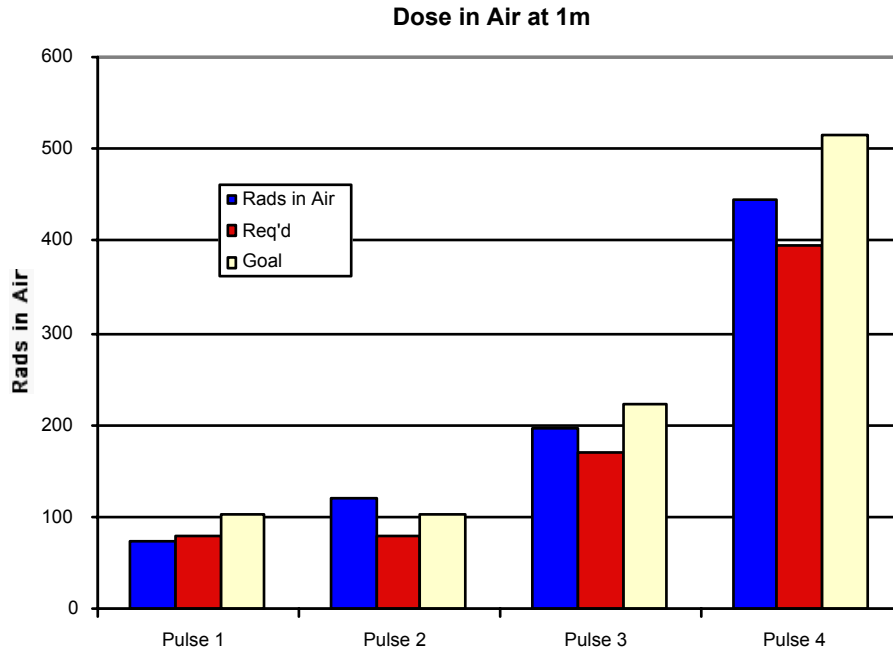


Figure 9. Dose from PIC-generated beam “swept” by kicker system.

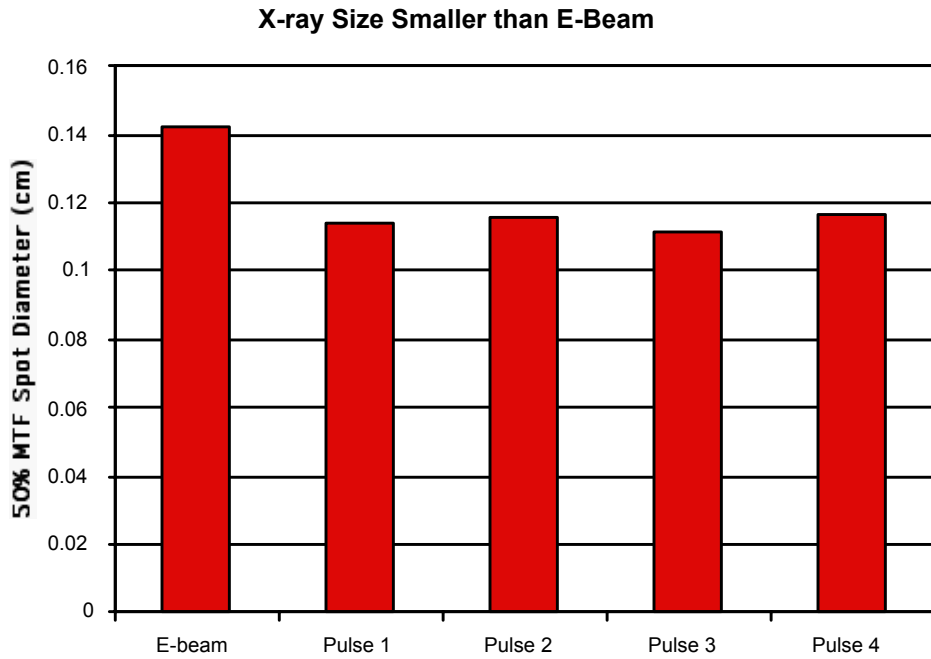


Figure 10. X-ray spot sizes for PIC-generated “swept” beam.

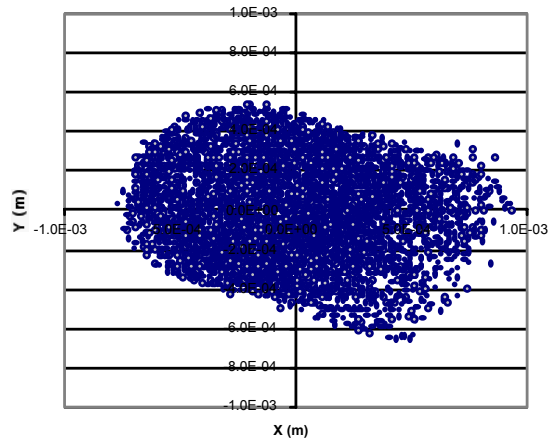


Figure 11. Physical space plot of “swept” beam on target; calcs by B. Poole.

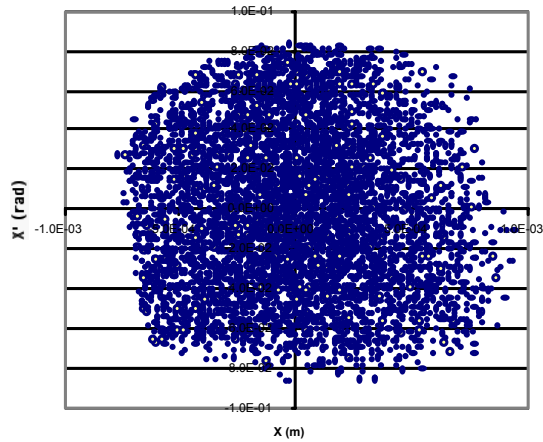


Figure 12. X-X' phase space plot of "swept" beam; this is the non-kicked plane. Calcs by B. Poole.

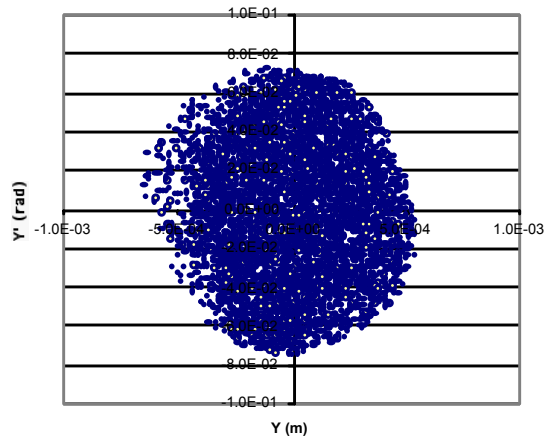


Figure 13. Y-Y' phase space plot of "swept" beam in the kicked plane. Calcs by B. Poole.

Sample MCNP Input File for Air Absorption Spectrum (15 MeV)

```

Dose curve for air
c Vacuum
1 0 -1:3:4          $ Outside everything
2 0 1 -2 -4        $ left edge to air
3 1 -1.225e-3 2 -3 -4 $ air
c end of cell cards

c Surfaces
1 PX -1.0 $ left boundary
2 PX 0.0 $ edge of air
3 PX 100.0 $ right boundary
4 CX 10.0 $ outer boundary
c End of surfaces

mode p
imp:p 0 1 1
cut:p 1.e37 0.001
fcl:p 0 0 -1
c 3456789012345678901234567890123456789012345678901234567890123456789012

```

```

c Source-----
sdef pos=-0.1 0.0 0.0 vec=1 0 0 dir=1 erg=15.0 par=2
c Tallies-----
f6:p 3
*f8:p 3
c Materials-----
M1 7000 0.7845 8000 0.2109 18000 0.0046 $ Air, density 1.225e-3 g/cc
NPS 500000

```

Sample MCNP Input File for Pulse 2

Dose, spot size, energy dep. from various DARHT targets

```

c Vacuum
1 0 -1:8:9 $ Outside everything
2 0 1 -2 -9 $ right edge to tamper
3 0 2 -3 -9 11 $ above 1st third of tamper
4 0 3 -4 -9 13 $ above middle of tamper
5 0 4 -5 -9 15 $ above end of tamper
6 0 5 -6 -9 $ tamper to knife edge
7 0 6 -7 16 -9 $ above knife edge
8 0 6 -7 -16 -9 $ knife edge
9 0 7 -8 -9 $ knife edge to boundary
10 0 2 -17 -10 $ source to target, inside tamper
11 0 27 -5 -14 $ target to tamper edge, inside tamper
c Tamper
12 1 -16.6 2 -3 10 -11 $ 1st third
13 1 -16.6 3 -4 12 -13 $ middle
14 1 -16.6 4 -5 14 -15 $ last third
c Target as radial profiles at various z
15 0 17 -18 -28 $ block before target: 1
16 0 17 -18 28 -29
17 0 17 -18 29 -30
18 0 17 -18 30 -31
19 0 17 -18 31 -32
20 0 17 -18 32 -10
21 0 18 -19 -28 $ block before target: 2
22 0 18 -19 28 -29
23 0 18 -19 29 -30
24 0 18 -19 30 -31
25 0 18 -19 31 -32
26 0 18 -19 32 -10
27 0 19 -20 -28 $ block before target: 3
28 0 19 -20 28 -29
29 0 19 -20 29 -30
30 0 19 -20 30 -31
31 0 19 -20 31 -32
32 0 19 -20 32 -10
33 1 -0.12 20 -3 -28 $ block before target: 4
34 1 -0.06 20 -3 28 -29
35 1 -5.2e-3 20 -3 29 -30
36 0 20 -3 30 -31
37 0 20 -3 31 -32
38 0 20 -3 32 -10
39 1 -1.6 3 -21 -28 $ block inside target: 1
40 1 -2.4 3 -21 28 -29
41 1 -7.0 3 -21 29 -30
42 1 -4.0 3 -21 30 -31
43 1 -3.95 3 -21 31 -32
44 1 -3.95 3 -21 32 -12
45 1 -2.0 21 -22 -28 $ block inside target: 2
46 1 -2.3 21 -22 28 -29
47 1 -5.3 21 -22 29 -30
48 1 -4.0 21 -22 30 -31
49 1 -3.95 21 -22 31 -32
50 1 -3.95 21 -22 32 -12
51 1 -2.0 22 -23 -28 $ block inside target: 3
52 1 -2.4 22 -23 28 -29
53 1 -5.4 22 -23 29 -30
54 1 -4.05 22 -23 30 -31
55 1 -3.95 22 -23 31 -32

```

```

56 1 -3.95 22 -23 32 -12
57 1 -2.3 23 -33 -28      $ block inside target: 4
58 1 -2.7 23 -33 28 -29
59 1 -4.9 23 -33 29 -30
60 1 -3.2 23 -33 30 -31
61 1 -4.0 23 -33 31 -32
62 1 -3.95 23 -33 32 -12
63 1 -3.0 33 -34 -28      $ block inside target: 5
64 1 -3.0 33 -34 28 -29
65 1 -4.4 33 -34 29 -30
66 1 -4.2 33 -34 30 -31
67 1 -4.0 33 -34 31 -32
68 1 -3.95 33 -34 32 -12
69 1 -3.4 34 -4 -28      $ block inside target: 6
70 1 -3.4 34 -4 28 -29
71 1 -4.2 34 -4 29 -30
72 1 -4.0 34 -4 30 -31
73 1 -3.95 34 -4 31 -32
74 1 -3.95 34 -4 32 -12
75 1 -3.0 4 -24 -28      $ block after target: 1
76 1 -2.9 4 -24 28 -29
77 1 -3.8 4 -24 29 -30
78 1 -3.9 4 -24 30 -31
79 1 -3.8 4 -24 31 -32
80 1 -2.8 4 -24 32 -14
81 0 24 -25 -28      $ block after target: 2
82 0 24 -25 28 -29
83 0 24 -25 29 -30
84 0 24 -25 30 -31
85 0 24 -25 31 -32
86 0 24 -25 32 -14
87 0 25 -26 -28      $ block after target: 3
88 0 25 -26 28 -29
89 0 25 -26 29 -30
90 0 25 -26 30 -31
91 0 25 -26 31 -32
92 0 25 -26 32 -14
93 0 26 -27 -28      $ block after target: 4
94 0 26 -27 28 -29
95 0 26 -27 29 -30
96 0 26 -27 30 -31
97 0 26 -27 31 -32
98 0 26 -27 32 -14
c end of cell cards

c Surfaces
1  PX  1.60 $ left boundary
2  PX  1.80 $ source surface, start of tamper
3  PX  2.53 $ left edge of t=0 targ
4  PX  2.95 $ right edge of t=0 targ
5  PX  3.40 $ right edge of tamper
6  PX 102.74 $ knife edge front
7  PX 102.75 $ knife edge back
8  PX 202.74 $ right boundary
9  CX  0.70 $ outer boundary
10 KX 11.63 2.717e-4 -1 $ Cones bounding first third of tamper
11 KX 17.70 2.717e-4 -1
12 KX  1.69 3.189e-2  1 $ Middle third of tamper
13 KX  1.13 3.189e-2  1
14 KX  2.25 0.1033 1      $ Last third of tamper
15 KX  1.95 0.1033 1
16 PY  0.00 $ Plane to split knife edge
17 PX  2.13 $ axial blocks, left of t=0 targ
18 PX  2.23
19 PX  2.33
20 PX  2.43
21 PX  2.60 $ axial blocks, inside t=0 targ
22 PX  2.67
23 PX  2.74
24 PX  3.05 $ axial blocks, right of t=0 targ
25 PX  3.15

```


202.739 0.03 0 0 202.739 0.05 0 0 202.739 0.07 0 0 202.739 0.09 0 0 &
202.739 0.11 0 0 202.739 0.13 0 0 202.739 0.15 0 0 ND
*f8:p,e 15 16 17 18 19 20
*f18:p,e 21 22 23 24 25 26
*f28:p,e 27 28 29 30 31 32
*f38:p,e 33 34 35 36 37 38
*f48:p,e 39 40 41 42 43 44
*f58:p,e 45 46 47 48 49 50
*f68:p,e 51 52 53 54 55 56
*f78:p,e 57 58 59 60 61 62
*f88:p,e 63 64 65 66 67 68
*f98:p,e 69 70 71 72 73 74
*f108:p,e 75 76 77 78 79 80
*f118:p,e 81 82 83 84 85 86
*f128:p,e 87 88 89 90 91 92
*f138:p,e 93 94 95 96 97 98
c Materials-----
M1 73000 1.0 \$ Ta, density 16.6 g/cc
NPS 500000